Experimental optical imaging during pancreatic cancer interventions

Manen, L. van

Chapter 6

Latest developments in molecular tracers for fluorescence image-guided cancer surgery

S. Hernot, L. van Manen, P. Debie, J.S.D. Mieog, A.L. Vahrmeijer

Lancet Oncology. 2019 Jul;20(7).

Abstract

Real-time intraoperative guidance is essential during oncological surgery for complete and safe tumour resection. Fluorescence imaging in the near-infrared spectrum has shown potential for guiding surgeons during complex interventions. Recently, there has been a shift towards the use of fluorescence contrast agents for molecular imaging. The first targeted fluorescent agents, of which most consist of approved therapeutic antibodies conjugated to a fluorescent dye, have been evaluated in several early-phase clinical trials. Moreover, advances in protein engineering and drug design have led to the development of a variety of tracers suitable for molecular fluorescence image-guided surgery. In this Review, we discuss preclinical and clinical evidence, ongoing clinical trials, and the latest developments in the field of molecular near-infrared tracers for fluorescence-guided cancer surgery.

Introduction

Surgery is pivotal in the treatment of solid cancers. Unfortunately, tumour-positive resection margins occur in 8-70% of the cases depending on the cancer type.[1-4] Because complete removal of tumour tissue is mandatory for prolonged survival and to preserve as much healthy tissue as possible, intraoperative guidance is essential to surgeons. Besides using visual (based on white light reflectance) and tactile feedback, surgeons can use ultrasound imaging as an additional tool for intraoperative guidance in selected cases, but this tool alone is often insufficient.[5] Other imaging techniques, such as x-ray, CT, or MRI are mainly used for surgical planning or interim assessment because they do not provide real-time intraoperative guidance. Recently, surgeons have started to use fluorescent light for surgical navigation.

Fluorescence imaging uses a specialised camera to capture light emitted by a fluorescent contrast agent after excitation with an appropriate light source. All imaging equipment can be integrated into a compact open-field device or within laparoscopic or robotic instruments for contact-free and real-time interrogation (Figure 1). The fluorescent contrast agent is administered to visualise the organ or tissue of interest with sufficient sensitivity and contrast. For medical applications, fluorescent agents that emit at wavelengths in the near-infrared region, between 650 and 800 nm, are more advantageous than those emitting visual light. Near infrared light can penetrate deeper into tissue (up to several mm) with less scattering than visual light and there is less autofluorescence.[6]

Indocyanine green and methylene blue are the only available near-infrared fluorophores that are approved by the US Food and Drug Administration. Indocyanine green is mainly used for the evaluation of blood flow, sentinel lymph node mapping, and liver tumour imaging.[7] Methylene blue has been evaluated for ureter, thyroid nodule, and neuroendocrine tumour visualisation; however, it is currently not used in regular surgical care due to its non-specificity and limited quantum yield. Besides indocyanine green and methylene blue, 5-aminolevulinic acid and its derivate 5-aminolevulinic acid hexyl ester, are two non-fluorescent prodrugs that are both clinically approved for imaging of malignant gliomas and bladder cancer, respectively. These prodrugs elicit the synthesis of fluorescent protoporphyrin IX (maximal emission peak around 634 nm, thus just outside the near-infrared region), which accumulates in malignant tumour tissue. Two randomised controlled phase 3 trials [8,9] have shown improved resection margins and also increased progression-free survival for patients with malignant gliomas and bladder cancer. However, drawbacks of fluorescence imaging with 5-aminolevulinic acid include inhomogeneous signals that are dependent on the tumour grade, absence of penetration depth, and photobleaching.[10]

Over recent years there has been a shift from structural and functional fluorescence imaging to molecular fluorescence imaging using more specific fluorescent agents (Figure 2). Molecular fluorescence imaging could be used for many applications relevant to oncological surgery such as the detection of occult tumour lesions, assessment of tumour margins and locoregional invasion, and emphasis on vital structures (Figure 1).[11] In this Review, we focus on the clinical evidence in molecular near-infrared fluorescence-guided cancer surgery and latest developments regarding molecular probes in the field.

Targeted fluorescent agents under evaluation in clinical trials

The specific accumulation of a fluorescent contrast agent in a tissue of interest requires stable conjugation of a fluorophore to a targeting molecule. The targeted cells, most often cancer cells, will thus literally light up, whereas the background is expected to be significantly less fluorescent once the unbound tracer has cleared. Several tumour-specific ligands, recognising diverse molecular biomarkers, have been evaluated for molecular fluorescence imaging applications in the clinic. An overview of published and ongoing clinical trials is provided in Table 1.

In 2011, van Dam and colleagues[12] did the first targeted fluorescence molecular imaging trial by using the contrast agent EC-17, which consists of folic acid conjugated with fluorescein isothiocyanate (emission: 520 nm), in patients with ovarian cancer during cytoreductive surgery. In three patients, folate receptor-alpha expressing malignant tumour deposits could be clearly identified intraoperatively and distinguished from benign structures. Similar results were found for lung, breast and renal tumours. [13-16] However, the limited penetration of light and relatively high autofluorescence signal arising from collagen-rich tissues in this wavelength range turned out to be suboptimal. Consequently, the analogous fluorescent tracer OTL-38, also targeting folate receptor, but emitting at 796 nm, was developed and tested in several cancer types including ovarian, lung, renal and endometrial tumours, as well as mengingioma.[17-26] Hoogstins and colleagues [17] showed in 12 patients with ovarian cancer that surgeons were able to detect 29% additional malignant lesions during debulking surgery, which were not detected using visual inspection. Other pilot studies showed that pulmonary adenocarcinomas could be detected with a sensitivity up to 100% [23] and squamous cell carcinomas with up to 70%.[21] Furthermore, in situ fluorescence imaging even appeared to be superior to 18F-FDG-PET for the detection of malignant pulmonary nodules.[19] A larger multicenter international phase 2 trial (NCT02872701) determining the clinical efficacy in terms of detection of additional tumour-positive nodules, synchronous lesions, and tumour-positive margins during lung surgery in 110 patients has been completed, but results are not published yet. In another trial, [26] endometrial cancer, including omental and lymph node metastases, could also be detected using OTL-38 in four patients. Nevertheless, a high rate of false-positive signals (34%) was recorded, which was caused by the non-specific targeting of OTL-38 to folate receptor-β in non-metastatic lymph nodes.

Alternatively, tozuleristide is a naturally occurring knotted peptide conjugated to indocyanine green. This tracer has known affinities for matrix metalloproteinase-2 and annexin A2, which are expressed in a variety of solid tumours. Dintzis and colleagues [43] showed that tozuleristide, when administered between 1 to 26 h before surgery, enabled detection of tumour tissue in freshly resected pathology specimens of 23 patients with breast cancer. Phase 1 studies (NCT02234297; NCT02462629) in paediatric and adult subjects with CNS tumours have been completed and a randomised phase 2/3 trial (NCT03579602) has started recruiting patients.

With the introduction of the commercially available near-infrared fluorophore IRDye800CW, existing therapeutic monoclonal antibodies could quite easily be repurposed after fluorescence labelling. For example, bevacizumab-IRDye800CW has been used in various clinical feasibility trials targeting tumours that overexpress vascular endothelial growth factor. Harlaar and colleagues [27] studied seven patients with peritoneal carcinomatosis of colorectal origin undergoing cytoreductive surgery and

showed that fluorescence imaging with bevacizumab-IRDye800CW enabled in-situ detection of additional malignant lesions while fluorescence uptake was absent in clinically suspicious but benign lesions. Contrarily, for breast cancer surgery, a dose of 4.5 mg of bevacizumab-IRDye800CW, which falls under the microdosing regimen, was too low to enable in-situ margin assessment.[28] Tumour-positive margins could nevertheless be detected *ex vivo* after bread-loaf slicing (a common method of processing surgical specimens for histopathology) on the back table.[28] These results demonstrate the relevance of developing fluorescence-guided intraoperative pathology that could provide fast feedback to the surgeon on excised specimens (Figure 1). However, detection of lymph node metastases was difficult. Additional studies with bevacizumab-IRDye800CW are planned in endometriosis (NCT02975219), pancreatic cancer (NCT02743975) and perihilar cholangiocarcinoma (NCT03620292).

According to an analogous strategy, the human-mouse chimeric monoclonal antibody cetuximab, which targets the epidermal growth factor receptor (EGFR), was conjugated to IRDye800CW.[29] Rosenthal and colleagues [30] reported no grade 2 or higher adverse events after administration of cetuximab-IRDye800CW in a dose-escalation study with doses up to 62.5 mg/m^2 which corresponds to 25% of the therapeutic dose of cetuximab, preceded by an injection of 100 mg of unlabelled cetuximab. Furthermore, in-situ mean target-to-background ratio values up to 5.2 were found between head and neck tumours and surrounding tissue. This study [30] also showed the ability of *ex vivo* back-table fluorescence imaging to identify positive tumour margins, as well as over resected lesions. Cetuximab-IRDye800CW yielded high sensitivity (97%) and specificity (93%) for the *ex vivo* detection of lymph node metastases compared with standard histopathology.[31] This finding suggests that unnecessary neck lymph node dissections could potentially be avoided, eventually resulting in decreased morbidity. A Phase 2 clinical trial has been launched in 70 patients with the aim to determine the fluorescent threshold level needed to distinguish tumour tissue from normal tissue (NCT03134846). Tummers and colleagues [33] evaluated the accuracy of the same tracer during pancreatic surgery in seven patients. A sensitivity of 96% and a specificity of 67% were achieved for primary tumour detection, with a mean in-situ target to background ratio value of 2.3. Tumour positive lymph nodes could also be identified intraoperatively (mean target to background ratio of 6.3). *Ex vivo* fluorescence analysis showed a sensitivity of 100% and specificity 78% macroscopically, and a sensitivity of 91% and specificity of 66% microscopically for detection of metastatic lymph nodes in the optimal dose cohort (50 mg).[34] Cetuximab-IRDye800CW has also been tested in three patients with glioblastoma, of which the two contrast-enhancing tumours on preoperative CT imaging showed fluorescence signal accumulation with a mean *ex vivo* TBR of 4.0, whereas the non-contrast-enhancing tumour did not show a clear fluorescence signal (ratio of 1.2).[35]

IRDye800CW-labeled panitumumab, which is a fully humanised monoclonal antibody with improved EGFR binding characteristics compared with cetuximab-IRDye800CW, was clinically evaluated in a dose escalation study [32] using a loading dose of 100 mg unlabelled panitumumab before surgery to saturate EGFR receptors in normal tissue and therefore optimize tissue contrast. Doses of 0.5 and 1 mg/kg allowed in-situ imaging of head and neck tumours with mean target to background ratios between 2.4 and 2.6. Fluorescence imaging was able to detect tumour tissue in the resected specimens with a high sensitivity of 91% and negative predicting value of 93%.[36] Further analysis of the back-table fluorescence imaging data yielded a 100% sensitivity for the

detection of tumour-positive resection margins (<2 mm) and 95% sensitivity for close resection margins (<5mm).[37] Furthermore van Keulen and colleagues [38] showed that fluorescence imaging using panitumumab-IRDye800CW could improve the surgical decision-making in three (21%) of 14 patients with head and neck cancer through the identification of close margins and unanticipated regions of primary disease. In-situ margin assessment has not yet been investigated, although this would be more beneficial for the surgeon to plan and perform the resection during the procedure under fluorescence guidance.

Finally, a 700 nm fluorophore conjugated to an anti-carcinoembryonic antigen (CEA) targeting antibody, SGM-101, was recently evaluated in two pilot studies for 26 patients needing colorectal cancer surgery and 12 patients who needed pancreatic cancer surgery. Tumour-specific fluorescence signals, with the highest target to background ratios (*in vivo* 1.8 and *ex vivo* 6.1) found in the 10 mg dose group, could be observed during surgery with a diagnostic accuracy of 84% in colorectal tumours.[40] In the expansion cohort comprising 17 patients, fluorescence imaging yielded 19 (43%) extra lesions compared with the surgeon's clinical evaluation, resulting in a change of treatment plan in 32% of the patients. In patients with pancreatic adenocarcinoma, fluorescence imaging using SGM-101 was able to detect 21 lesions in total, of which one was a false-positive.[39] However, because of the presence of dense desmoplastic stromal tissue surrounding tumour ducts, fluorescence signals and associated target to background ratios were more modest compared with the colorectal cancer group (*in vivo* 1.6 and *ex vivo* 3.2). Two lesions detected by visual inspection were not fluorescent. The use of SGM-101 could have resulted in a change of the treatment plan in one patient, as illustrated in Figure 3.

Hybrid fluorescent and radioactive targeted tracers

To overcome the main limitation of near-infrared fluorescence image guidance in terms of the sensitive detection of deeper-lying lesions, use of multimodality imaging has been advocated. Nuclear techniques have been found to be particularly complementary with fluorescence navigation because gamma rays are scarcely attenuated by overlying tissue. In addition to the superficial fluorescent signal, contrast agents featuring both a radioactive label and a fluorescent dye can offer preoperative information for surgical planning via single photon emission computed tomography or PET imaging and acoustic guidance for the surgeon via gamma-probe tracing. ^{99m}Tc-Nanocolloid in complex with indocyanine green was the first hybrid tracer tested in humans for refinement of the sentinel lymph node procedure. A prospective trial of 495 patients with head and neck cancer, skin, penile, prostate or vulva cancer, showed the benefit of indocyanine green-^{99m}Tc-Nanocolloid in terms of precise visual guidance, depth estimation and detection of sentinel lymph nodes close to the injection site.[49] However, the intraoperative detection of (lymph node) metastases or occult tumour lesions requires targeted agents.

The monoclonal antibody girentuximab-IRDye800CW co-labelled with ^{111}In was used for the visualisation of clear-cell renal-cell carcinomas, in which carbonic anhydrase IX is overexpressed. [41] Fluorescence imaging was feasible in 12 patients, with high fluorescence in the tumour (mean

target to background ratio of 2.5). The added-value of the radioguidance consisted in tracing lesions covered with perinephric fat and endophytic lesions. Bombesin, co-labelled with IRDye800CW and ^{68}Ga was used in 14 patients for detection of glioblastoma multiforma in which the gastrin-releasing peptide receptor is overexpressed. Good correlation between PET signals and intraoperative fluorescence signal was shown. During surgery, most of the tumours showed fluorescence (mean target to background ratio of 4.9), resulting in a sensitivity of 94% and specificity of 100%.[42] With the recent success of radiolabelled prostate-specific membrane antigen (PSMA)-targeted tracers for PET/CT imaging and targeted radionuclide therapy, efforts have also been made towards the design and preclinical validation of hybrid nuclear and fluorescent PSMA-tracers for use as surgical navigation tools in prostate cancer.[50]

Activatable fluorescent agents evaluated in clinical trials

A different strategy to actively trace tumour tissue is by using activatable fluorescent tracers. The fluorescent agent is optically silent until activated, often through enzymatic cleavage of the backbone structure (Figure 2). Two activatable fluorescent probes, LUM015 and AVB-620, have been evaluated clinically. Whitney and colleagues [44] described the use of LUM015, which is a cathepsin-activated fluorescent probe, in a phase 1 study in 15 patients with sarcoma or breast cancer. LUM015 was well-tolerated in the three dose groups (0.5 mg/kg, 1.0 mg/kg and 1.5 mg/kg) and showed tumour-specific fluorescence during *ex vivo* imaging with a mean target to background ratio of 4.1 in 13 (87%) patients. Another research group showed the feasibility of LUM015 for intraoperative detection of residual breast cancer in 15 patients.[45] In this cohort, elevated fluorescent signals were noticed in *ex vivo* resected breast tumours, resulting in mean target to background ratios of 4.7 in the 0.5 mg/kg group, and 4.2 in the 1.0 mg/kg dose group. Furthermore, for five patients, residual positive margins could be detected in the lumpectomy wall. Currently, a phase 2 study (NCT03321929) is recruiting patients with breast cancer to determine the efficacy of LUM015 in a larger patient cohort (n=250) and a phase 3 trial (NCT03686215) will start soon afterwards. Next to this, LUM015 is also being evaluated for detection of other cancer types such as gastrointestinal cancers (NCT02584244), peritoneal metastasis (NCT03834272), brain cancer (NCT03717142), or prostate cancer (NCT03441464).

The first clinical use of AVB-620, in breast cancer was described by Unkart and colleagues.[46] This tracer consists of a cell-penetrating peptide bearing a Cy5 fluorophore and a neutralising peptide bearing a Cy7 fluorophore. After proteolytic cleavage, the two peptides are separated, and the Cy5 bearing cell-penetrating peptide will become functional, increasing Cy5 fluorescence intensity and decreasing Cy7 emission. The Cy5/Cy7 fluorescence ratio was used for the analysis of fluorescence signals on resected tumour specimens. 15 patients were included in a dose-escalation cohort and 12 patients in the expansion cohort. Depending on injection time, either 1 day before surgery or on the day of surgery, mean fluorescence ratios of *ex vivo* tumour specimens obtained were 1.1 or 1.9 for cancerous breast tissue, and 0.6 or 1.2 for adjacent normal breast tissue. Based on these results a phase 2 trial (NCT03113825) has been launched to determine the accuracy of AVB-620 for distinguishing malignant and nonmalignant breast tissue.

Emerging targeted fluorescent molecular tracers with improved pharmacokinetics and specificity

The inherent capacity of antibodies to effectively recognise specific cell-surface expressed antigens and the relatively easy process through which new antibodies can be generated, makes them the biggest class of readily available targeted agents. Therefore, many groups are currently evaluating preclinically novel near-infrared fluorescence-labelled antibodies targeting alternative biomarkers for distinct intraoperative imaging applications, all showing the feasibility of the antibodies to highlight tumour lesions.[51-54] The long blood retention of antibodies due to their large size and neonatal Fc receptor-mediated recycling, in combination with the enhanced permeability and retention effect has been associated with long delayed imaging times (several days between the moment of injection and the surgery) and non-specific tissue accumulation resulting in false positive signals.[33,40,55] Furthermore, antibodies are known to show poor tissue penetration at microscopic level (Table 2).[56]

Advances in protein-engineering have led to the development of antibody-fragments (minibodies, Fab-fragments, diabodies,[57] and single chain variable fragments) (Figure 2, Table 2) that retain similar binding characteristics, but show better tumour penetration and more rapid clearance from non-targeted tissues. For example, Zhang and colleagues [58] showed that the IRDye800CW-labelled minibody that is specific to the prostate stem-cell antigen facilitated complete resection of invasive tumours and detection of tumour-infiltrated lymph nodes in mice. A clinical trial with the minibody IAB2M-IRDye800CW that is specific to prostate specific membrane antigen has been launched with the aim of evaluating the safety, feasibility, and optimal dose of the contrast agent to visualise cancer invasion in 20 patients. In a second stage, the effect of fluorescence imaging guidance on the completeness of tumour resection, urinary and sexual function outcome, disease recurrence, and survival will also be assessed in 50 men who are scheduled for robot-assisted laparoscopic radical prostatectomy (ISRCTN10046036).

Antibody-fragments with a low molecular weight (<60 kDa in size) that are rapidly eliminated from the blood via renal excretion have especially been researched as tools for molecular imaging applications because they enable highly specific and high-contrast imaging at early timepoints after injection.[59] However, the conjugation of near-infrared fluorescent dyes (such as IRDye800CW) can cause increased albumin binding and hepatic clearance of the tracers, and that can possibly influence their typical pharmacokinetic profile.[60] The Fab-fragment VB6–845-IRDye800CW, which targets the epithelial cell adhesion molecule highly overexpressed on most epithelial cancers, showed high target to background ratios between 8 and 24 h after injection in orthotopic breast and colorectal tumour mouse models.[61] This tracer has been produced for clinical use and a phase 1 trial (NL7363) is planned in patients with oesophageal, gastric, or rectosigmoid cancer who will have laparoscopic surgery. Researchers have also been interested in single- domain antibodies, better known as nanobodies™, which are derived from heavy-chain antibodies found in camelids. Several fluorescently-labelled nanobodies, targeting tumour markers such as carbonic anhydrase IX or HER2 have been successfully evaluated in preclinical models, with noteworthy tumour to background ratios reached within 1 to 3 h after injection.[62,63]

Another class of targeted agents that have elicited interest are non-immunoglobulin protein scaffolds, which include centyrins, affibodies, or cystine knottins (Figure 2).[64–66] These scaffolds exhibit similar pharmacokinetics as the small antibody fragments, but are generated through random mutagenesis or rational design of the antigen-binding regions, instead of via immunisation in which the affinity of molecules for their antigen is matured naturally in an animal. For example, the IRDye800CW-labelled anti-EGFR affibody molecule ABY-029 showed high-uptake and high-contrast values on *ex vivo* slices compared with normal brain tissue in an intracranial glioma rat model within 1 h after injection.[67] ABY-029 is under investigation in three phase 1 clinical trials; one for recurrent glioma (NCT02901925), another for primary sarcoma (NCT03154411), and one in head and neck cancer surgery (NCT03282461). In addition to the clinically tested tozuleristide, Tummers and colleagues [65] validated another cystine knottin peptide binding specifically to integrin $\alpha_v\beta_6$ in orthotopic and spontaneous transgenic pancreatic tumour models.

Peptides and small molecules are even smaller in size than the compounds above; however, the pharmacokinetic profile of each tracer becomes dependent on their individual physicochemical characteristics. In comparison with platform technologies such as antibodies, antibody fragments, and protein scaffolds high throughput generation of novel peptides and small molecules with adequate properties for *in vivo* imaging is more difficult and unpredictable. However, once a lead compound against a specific biomarker has been identified, it can be routinely produced according to current good manufacturing protocols for clinical use at a much lower cost than biologicals, which require production through fermentation (Table 2). Bombesin-antagonists [68] and RGD peptides [69] are often subject to preclinical investigation. Besides IRdye800CW and Cy5, cRGD has also been conjugated with zwitterionic fluorophore ZW800–1. cRGD-ZW800–1 exhibits substantially less non-specific binding in normal organs and tissues than does IRDye800CW-labelled cRGD, and is cleared exclusively through the kidneys.[70] A drawback of ZW800–1 is its instability over time in serum, although it appears that this limitation can be overcome by rapid internalisation.[71] Using cRGD-ZW800–1, Handgraaf and colleagues [69] showed the feasibility to image integrin overexpression on malignant and neoangiogenic cells in various tumour models, including pancreas, colorectal, oral, and breast cancer with high tumour signals and tumour to background ratios at 4 h after injection. Moreover, tumour signals were still clearly distinguishable after 24 and even after 48 h. Because of the easy production procedure and low cost, this probe is undergoing clinical translation and the first human data are expected in the near future (NL7724; Table 1).

Challenges and considerations towards clinical translations of novel tracers

A wide variety of molecular tracers have shown potential to specifically highlight tumour lesions in animal models and are awaiting clinical translation. The field of PET imaging, which is considerably more advanced regarding the development of targeted tracers, favours the use of highly specific agents with fast pharmacokinetics, both from a safety and practical point of view. Analogously, for fluorescence imaging applications, the timing of administration of the contrast agent (e.g., just before surgery would be highly convenient) and the clearing pattern of the agent need to be considered. For example, renally cleared agents would permit improved visualisation of liver lesions in comparison with fluorescent agents cleared via the hepatobiliary route.[59] However, because the minimal signal level that must be reached for sensitive detection with fluorescence imaging devices is higher than for PET, slower blood clearance rates could enhance signal intensities at the target. Dose optimisation studies are therefore essential to obtain superior image quality in terms of both signal intensity and tumour to background ratios. Yet, the use of highly sensitive imaging instruments and the design of brighter fluorescent dyes are probably more advisable approaches towards clinical translation than increasing the injected dose of rapidly cleared targeted contrast agents to improve detection's sensitivity because of potential toxicity.

Despite all preclinical evidence, the real assessment of the value of fluorescent contrast agents for intra-operative imaging can only be performed in humans. Hereto, promising compounds have to undergo a translational process before clinical trials can be initiated. Current good manufacturing practice and toxicity studies remain the main bottlenecks of development because of their cost and time-consuming administrative burden. Because targeted fluorescent contrast agents often require doses above the microdosing level, a simplified regulation with less extensive toxicity studies as for radiopharmaceuticals is unfortunately not possible. Fast clearing tracers with predictable biodistributions could eventually have an advantage regarding documentation of the intended use because they are less likely to elicit unpredictable toxicity issues. Furthermore, the choice for a targeting moiety will have to be balanced between the ease of generation (derived from a generic platform technology) and the cost for routine production (relatively cheap chemical synthesis *vs* expensive fermentation process). For the field of intraoperative fluorescence imaging, this is even more important because the financial added value is probably less than for cancer therapeutics or companion diagnostic PET tracers.

The effectiveness of a molecular tracer will not only be determined by its general pharmacokinetic profile but will also be highly dependent on the biomarker it is intended to recognise and its expression pattern. Unfortunately, so far, no clear consensus exists on the most optimal biomarkers for the field. Yet, many prerequisites have been defined; these include: the biomarker should be highly overexpressed on tumour cells or stroma, while presenting no or low expression on normal tissue or after chemotherapy or radiotherapy to ensure high-contrast and specific imaging of only the tissue of interest; biomarkers are preferred to be extracellularly expressed to permit targeting by molecules that do not penetrate cells, but should ideally also internalise after binding for a long-lasting signal; the biomarker should show specificity across at least different types and subtypes of cancers to avoid preoperative screening of patients (unlike nuclear medicine applications for which

lately targeting of highly specific biomarkers is most often warranted to enable patient stratification for personalised therapies); and within one tumour type, homogeneous expression throughout the cancerous tissue is warranted, independently of tumour stage. However, most human tumours are known to exhibit substantial spatial and temporal intratumour heterogeneity, and this aspect is particularly difficult to mimic in preclinical models. Therefore, *in vivo* efficacy shown in preclinical research can often not be directly extrapolated to the clinical setting. From a regulatory and economic point of view, the feasibility of administrating a cocktail of fluorescent molecular tracers to overcome tumour heterogeneity has been suggested but is unlikely.

Future perspectives

Intraoperative fluorescence molecular imaging is still in its infancy. Clinical studies completed so far mainly consist of early-phase trials aimed at evaluating the safety of fluorescent contrast agents, estimating the optimal dose, showing feasibility of intraoperative lesion detection, and assessing exploratory data on sensitivity and specificity. It has been shown that near-infrared fluorescence imaging can improve the detection of peritoneal lesions during cytoreductive surgery, which is associated with improved survival. However, the primary solid tumour types for which surgical margin assessment and intraoperative staging (i.e., detection of lymph node or distant metastases) would be most beneficial, is not yet established. On the one hand, depending on the desired distance of the resection margin, in-situ molecular fluorescence imaging could be supportive to plan surgical dissection planes or to visualise remnant tumour cells after resection. On the other hand, surgical specimen imaging could be complementary and could provide precise information about both the extent of the tumour and the resection margins. When close resection margins are encountered, an additional resection could be considered and performed.

Large, multicentre, randomised controlled trials are thus mandatory to find out the diagnostic accuracy of fluorescence molecular imaging and to show the value of this technique on surgical outcomes and benefits to the patient. To convince regulatory authorities and reimbursement agencies, it is essential to identify clinically meaningful endpoints and surrogates of clinical benefit that are acceptable to authorities. A phase 3 multicentre, randomised controlled trial (NCT03659448) has been launched in patients with metastastic colorectal cancer to prove the added value of imaging with SGM-101 targeting anti-carcinoembryonic antigen in terms of resection margins. Furthermore, a phase 3 trial (NCT03180307) with OTL-38 is underway and includes patients with ovarian cancer who are scheduled to have open debulking surgery. In this study, the efficacy, which has been defined as the proportion of patients in which fluorescence imaging yields at least one additional tumour-positive lesion compared with normal conditions, will be assessed, as well as the diagnostic accuracy of OTL-38 at the patient level.

Nevertheless, the absence of a general consensus on standardised protocols for the clinical evaluation of new molecular fluorescent agents makes the conduction of multicentre trials and the comparison between clinical studies difficult. For example, tumour to background ratio is an important determinant for evaluating the efficacy of a fluorescent tracer; however, calculating

tumour to background ratios could be influenced by selection bias of relevant regions of interest, and studies report tumour to background ratios measured in different circumstances (e.g., *in vivo* or *ex vivo*). Furthermore, detected signal intensities not only depend on the chemical, photo- chemical, and biological characteristics of the fluorescent agent being investigated; but are also affected by tissue optical factors, depth of signal, as well as by the technical specifications and performance of the chosen imaging instrument. Importantly, the fluorescence imaging system should match the fluorescent contrast agent for optimal detection. Despite considerable efforts towards the development of a universal tool for calibration, quality control, and benchmarking of imaging devices, its development remains challenging because of the diversity of parameters influencing imaging.[72] Alternatively, advances in methods and models supporting accurate quantification of fluorophore concentrations in tissue would enable more objective distinction between tumour or non-tumour tissue. Improved image processing and interpretation would be desirable for the determination of clinically relevant cut off values for resection margins and exclusion of false-positive signals.[73] Meanwhile, guidelines regarding experimental workflow, data collection, image analysis, and reporting have emerged.[74–76] These are intended to obtain reliable, reproducible, and comparable data that will eventually ensure clinical implementation and approval of the technique.

Besides adequate open-surgery fluorescent imaging devices currently available, many laparoscopic and robotic surgical systems are already equipped with fluorescence cameras. It is to be expected that, in the future, more and more complex surgeries will be performed in a minimally invasive way, because they have already shown substantial benefits and led to a reduction in hospital costs.[77] With minimally invasive surgeries, it is even more important to guide the surgeon because of the limited field of view, associated risk of missing hidden lesions, and the absence of tactile feedback. However, it is also important to simultaneously highlight vital structures such as ureters or nerves, in addition to tumour tissue. During such procedures, the combination of fluorophores would be beneficial (e.g., one for tumour detection and one for detection of other important structures or tissue perfusion). This can be achieved by using fluorescence camera systems that are equipped with two or more fluorescent channels.

Conclusions

Fluorescence molecular imaging has so far shown its potential to support surgical procedures and the feasibility to improve clinical outcomes. Although there is much enthusiasm about these first results, intraoperative fluorescence molecular imaging is now at a crucial turning point in which unequivocal efficacy studies are needed to move the field beyond current proof of concept studies to produce a real change in clinical practice. Once this step has been taken, more extensive investments are to be expected towards novel tracers with improved characteristics pertaining to pharmacokinetics and specificity, as well as more sophisticated image analysis software. An important asset of fluorescence imaging is the relative ease by which the technology can be integrated within the routine of many different surgical and interventional cases, hence the necessity for centres of expertise to train users, as well as to create wide-spread awareness of the technique.

Figure 1. Principle of intraoperative molecular near infrared (NIR) fluorescence imaging. Top: Schematic illustration of (potential) applications of molecular targeted NIR fluorescence imaging. Bottom: Implementation of fluorescence guidance during both open and laparoscopic surgery. After intravenous injection of the tracer (one hour up to several days before surgery depending on the tracer), the tumour and/or other tissues-of-interest can be visualized with a specialized NIR camera, thereby guiding the surgeon in real-time during the resection. Immediately after resection, the specimen(s) can be sliced and imaged with a back-table fluorescence camera and microscope. The pathologist can thus rapidly check the resection margins on the presence of fluorescence and provide rapid feedback to the surgeon.

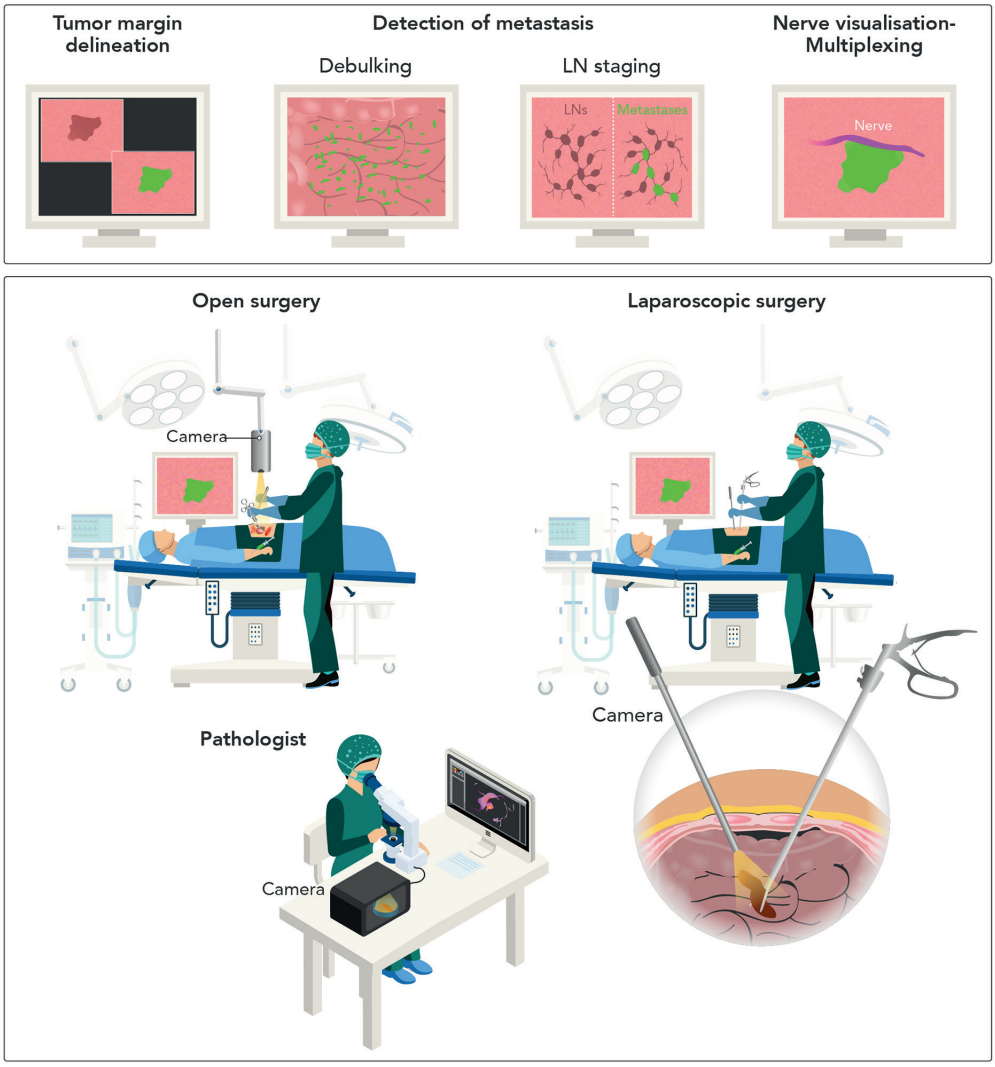

Figure 2. Molecular fluorescent contrast agents and targeting moieties used for intraoperative imaging during cancer surgery. Top: Schematic representation of the mode of action of the different types of fluorescent contrast agents. Non-targeted fluorescent contrast agents such as ICG aggregate to serum proteins in the circulation and passively accumulate in tumour tissue via the enhanced permeability and retention (EPR) effect. Targeted fluorescent contrast agents, consisting of a fluorescent dye conjugated to a targeting moiety, actively accumulate in tumour tissue by recognition of a specific biomarker expressed by tumour cells or tumour-associated stromal cells. Imaging is performed once unbound tracers have been cleared sufficiently. Activatable fluorescent contrast agents remain optically silent until fluorescent dyes are released by enzymatic digestion of their backbone. Bottom: Schematic representation of the different (sub-) classes of targeting moieties used for the design of targeted fluorescent contrast agents: Antibodies, antibody-fragments, protein scaffolds, peptides and small molecules. Representative space-filling images of an Antibody (1IGT), Fab (6B9Z), Diabody (1MOE), scFv (1P4I), Nanobody (5MY6), Centyrin (5L2H), Affibody (2KZJ) and Knottin (2N8B) were obtained from the RCSB protein bank and prepared using PyMOL. The space-filling Minibody model is an interpretation created using PyMOL, Antigen-binding regions are highlighted in orange.

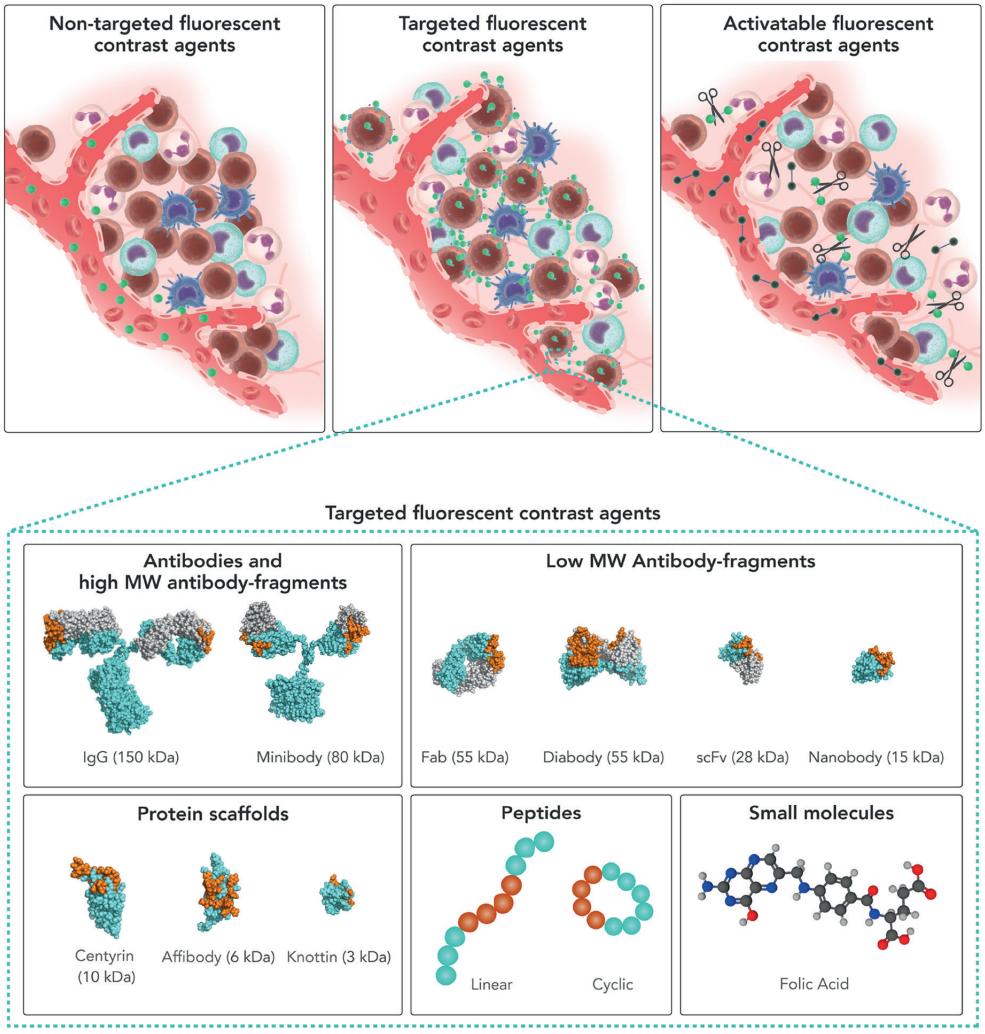

Table 1. Overview of ongoing and published clinical trials in molecular fluorescence-guided cancer surgery. Some studies share (partially) the same patient population. *VATS=video-assisted thoracoscopic surgery. VEGF=vascular endothelial growth factor. EGFR=epidermal growth factor receptor. CEA=carcinoembryonic antigen. CAIX=carbonic anhydrase IX. GRPR=gastrin-releasing peptide receptor. EpCam=epithelial cell adhesion molecule. PSMA=prostate-specific membrane antigen. HER2=human epidermal growth factor receptor 2. MMP=matrix metalloproteinase. HSP=heat shock protein. SPECT= single photon emission computed tomography. PEGylated=attachment of polyethylene glycol.*

Agent	Target	Ref or Study	Target tissue	Study type	Study population (n)	Incorporation	Interval between injection and surgery	Other(s)
EC17	Folate receptor	[12]	Ovarian cancer	Phase 1	10	Open (cytoreductive) surgery	2-8 h	..
		[13]	Lung cancer	Phase 1	30	Open surgery/ VATS	4 h	..
		[14]	Lung cancer	Phase 1	50	Open surgery	4 h	..
		[16]	Renal cell carcinoma	Case report	4	Open surgery	4 h	..
		[15]	Breast and ovarian cancer	Phase 1	15 (12 ovarian, 3 breast cancer)	Open surgery	2-3 h	..
		NCT01778933	Renal cell carcinoma	Phase 1	10	Open / laparoscopic surgery	2-4 h	..
OTL38	Folate receptor	[17]	Ovarian cancer	Phase 1a/Ib	42	Open (debulking) surgery	2-3 h	Phase 1a: 30 healthy volunteers Phase 1b: 12 patients
		NCT03180307	Ovarian cancer	Phase 3	147	Open (debulking) surgery	N.S.	..
		[18]	Renal cancer	Case report	3	Robotic surgery	2 h	..
		NCT02645409	Renal cancer	Phase 2	20	N.S.	2 h	..
		[19]	Pulmonary adenocarcinoma	Phase 1	50	VATS, robotic surgery	3-6 h	Combined with PET-CT
		[20]	Pulmonary adenocarcinoma	Case report	1	VATS	3-6 h	..
		[21]	Pulmonary squamous cell carcinoma	Phase 1	12	VATS	3-6 h	..
		[22]	Pulmonary adenocarcinoma	Phase 1	20	VATS	3-6 h	..
		[23]	Pulmonary adenocarcinoma	Phase 1	10	VATS	3-6 h	..
		[24]	Pulmonary ground glass opacities	Phase 1	20	VATS	3-6 h	..
		NCT02872701	Pulmonary adenocarcinoma	Phase 2 (multicenter)	110	VATS	2-3 h	..
		[25]	Meningioma	Case report	1	Open surgery	N.S.	..
		[26]	Endometrium	Phase 1	4	Open surgery	2-3 h	..

Agent	Target	Ref or Study	Target tissue	Study type	Study population (n)	Incorporation	Interval between injection and surgery	Other(s)
Bevacizumab-IRDye800CW	VEGF	[27]	Colorectal peritoneal metastases	Phase 1	7	Open surgery	2 days	..
		[28]	Breast cancer	Phase 1	20	Open surgery	3 days	..
		NCT02975219	Endometriosis	Phase 1	10	N.S.	3 days	..
		NCT02743975	Pancreatic cancer	Phase 1/2	26	Open surgery	3 days	..
		NCT03620292	Perihilar cholangio-carcinoma	Phase 1/2	12	Open surgery	3 days	Including *ex vivo* endoscopic fluorescence imaging of resected specimen
Cetuximab-IRDye800CW	EGFR	[29]	Head and neck cancer	Phase 1	9	Open surgery	3-7 days	Dose escalation study
		[30]	Head and neck cancer	Phase 1	12	Open surgery	3-7 days	Dose escalation study
		[31]	Head and neck cancer	Phase 1	12	Open surgery	3-7 days	Dose escalation study
		[32]	Head and neck cancer	Phase 1a	12	Open surgery	1-5 days	Dose escalation study evaluating both cetuximab-IRDye800CW and panitumum-ab-IRDye800
		NCT03134846	Head and neck cancer	Phase 1/2	79	Open surgery	4 days	Part I: dose escalation in 9 patients
		[33]	Pancreatic cancer	Phase 1	7	Open and laparoscopic surgery	2-5 days	Part 2: expansion cohort in 70 patients
		[34]	Pancreatic cancer	Phase 1	7	Open surgery	2-5 days	Photoacoustic imaging was also performed
		[35]	Glioblastoma	Case reports	3	Open surgery	2 days	..
Panitumum-ab-IRDye800CW	EGFR	[32]	Head and neck cancer	Phase 1a	15	Open surgery	1-5 days	Dose escalation study evaluating both cetuxi-mab-IRDYe800CW and panitumum-ab-IRDye800
		[36]	Head and neck cancer	Phase 1	21	Open surgery	1-5 days	..
		[37]	Oral squamous cell carcinoma	Phase 2	8	Open surgery	1-4 days	..
		[38]	Head and neck cancer	Phase 1	14	Open surgery	1-5 days	..
		NCT03384238	Pancreatic cancer	Phase 1/2	24	Open/ laparo-scopic surgery	2-5 days	..
		NCT03510208	Malignant glioma	Phase 1/2	22	Open surgery	1-5 days	..
		NCT03582124	Lung carcinoma	Phase 1/2	30	N.S.	1-5 days	..
		NCT03405142	Head and neck cancer	Phase 2	20	Open surgery	2-5 days	Focussing on lymph node detection by comparing near infrared fluores-cence with lymphoscintigra-phy and SPECT/CT after injection of 99mTc-labeled Tilmanocept

Agent	Target	Ref or Study	Target tissue	Study type	Study population (n)	Incorporation	Interval between injection and surgery	Other(s)
SGM-101	CEA	[39]	Pancreatic cancer	Phase 1	12	Open surgery	2-4 days	..
		[40]	Colorectal cancer	Phase 1/2	26	Open and laparoscopic surgery	2-4 days	..
		NCT03659448	Colorectal cancer	Phase 3 (Randomized controlled trial)	300	Open and laparoscopic surgery	2-4 days	..
^{111}In-DOTA-Labetuzumab-IRDye800CW	CEA	NCT03699332	Colorectal peritoneal metastases	Phase 1/2	29	Open surgery	6-7 days	Dual modality imaging
^{111}In-DOTA-Girentuximab-IRDye800CW	CAIX	[41]	Renal cancer	Phase 1	15	Open surgery	7 days	Dual modality imaging
^{68}Ga-NOTA-IRDye-800CW-BBN	GRPR	[42]	Glioblastoma	Phase 1	14	Open surgery	2 h	Dual modality imaging
Tozuleristide (BLZ-100)	Cell-surface chlorotoxin binding proteins	[43]	Breast cancer	Phase 1	23	Open surgery	1-26 h	Fluorescence imaging was only conducted ex vivo on resected specimens
		NCT02234297	Glioma	Phase 1	17	Open surgery	2 h	..
		NCT02462629	CNS tumours	Phase 1	32	Open surgery	1 h	Dose escalation and expansion cohort in pediatric subjects
		NCT03579602	CNS tumours	Phase 2/3 (randomized controlled trial)	114	Open surgery	1-36 h	Subjects will be randomized 1:10 to 1 of 2 study arms. Study arm 1: no BLZ-100 injection, although imaging will be performed. Study arm 2: BLZ-100 injection and imaging will be done.
VB5-845D-800CW	EpCam	NTR7570	Esophageal/gastric- or rectosigmoid cancer	Phase 1	34	Laparoscopic surgery	Optimal injection time will be based on the results of part Ia	Part Ia: dose escalation in human volunteers (N=16)
ABY029	EGFR	NCT02901925	Recurrent glioma	Phase 1a	12	Open surgery	1-3 h	..
		NCT03154411	Sarcoma	Phase 1a	18	Open surgery	1-3 h	..
		NCT03282461	Head and neck cancer	Phase 1a	12	Open surgery	1-3 h	..
IR800 IAb2M	PSMA	ISRCTN 10046036	Prostate cancer	Phase 1	120	Robot-assisted laparoscopic surgery	1-2 days	Part I: dose escalation in 20 patients Part 2: randomized allocation of IR800 IAb2M in 100 patients
cRGD-ZW800-1	Integrins (associated with tumor angiogenesis)	NL7724	Colorectal cancer	Phase 2	12	Laparoscopic surgery	<24 h	Ureter could also be visualized simultaneously, due to characteristics of ZW800-1

Agent	Target	Ref or Study	Target tissue	Study type	Study population (n)	Incorporation	Interval between injection and surgery	Other(s)
HS-196	HSP-90 inhibitor	NCT03333031	Breast cancer	Phase 1	120	Open surgery	24 h	Part I: dose escalation Part 2: expansion cohort
KSP-910638G	HER2	NCT03161418	N.S.	Phase 1a	26	N.S.	N.S.	Orally administration of tracer; safety trial in human volunteers
LS301	$\alpha_v\beta_3$ integrins	NCT02807597	Breast cancer	Phase 1	22	Open surgery	4-24 h	Including evaluation of feasibility for sentinel lymph node detection
LUM015	Cathepsins	[44]	Sarcoma and breast cancer	Phase 1	15	Open surgery	2-6 h	Activatable tracer: PEGylated protease-activated
		[45]	Breast cancer	Phase 2	15	Open surgery	2-6 h	Activatable tracer: PEGylated protease-activated
		NCT03321929	Breast cancer	Phase 2	250	Open surgery	2-6 h	Activatable tracer: PEGylated protease-activated
		NCT03686215	Breast cancer	Phase 3	250	Open surgery	2-6 h	Activatable tracer: PEGylated protease-activated
		NCT02584244	Colorectal, pancreatic, and esophageal cancers	Phase 1/2	21	Open surgery	2-6 h	Activatable tracer: PEGylated protease-activated; Fluorescence imaging will only be conducted ex-vivo on resected specimens
		NCT03834272	Peritoneal metastases	Phase 1	18	Open surgery	2-6 h	Activatable tracer: PEGylated protease-activated
		NCT03717142	Brain cancer	Phase 1	36	Open surgery	2-6 h	Activatable tracer: PEGylated protease-activated
		NCT03441464	Prostate cancer	Phase 1	12	Open surgery	2-6 h	Activatable tracer: PEGylated protease-activated; Fluorescence imaging will only be conducted ex-vivo on resected specimens
AVB-620	MMPs	[46]	Breast cancer	Phase 1	27	Open surgery	2-20 h	Activatable tracer: ratiometric activatable cell-penetrating peptide; Part I: dose escalation in 15 patients Part 2: expansion cohort of 12 patients
		NCT02901925	Breast cancer	Phase 2	110	Open surgery	< 24 h	Activatable tracer: ratiometric activatable cell-penetrating peptide

Growth Factor; EGFR: Epidermal Growth Factor Receptor, CEA: CarcinoEmbryonic Antigen, CAIX: Carbonic Anhydrase IX; GRPR: Gastrin-Releasing Peptide Receptor; EpCam: Epithelial Cell Adhesion Molecule; PSMA: Prostate-Specific Membrane Antigen, HER2: Human Epidermal Growth Factor Receptor 2; MMP: Matrix Metalloproteinase.

Figure 3. Example of intraoperative molecular fluorescence imaging during pancreatic surgery. A: Intraoperative fluorescence imaging of a pancreatic tumour (asterisk: tumour bulk), which could be visualized using a monoclonal antibody for carcinoembryonic antigen (CEA) conjugated to a 700 nm fluorophore (SGM-101). Based on the fluorescence image, the surgeons initially decided to move the planned resection line (black dashed line: proposed resection line based on visual inspection/palpation; blue dashed line: proposed resection line based on fluorescence). B: *Ex vivo* analysis of a resected pancreatic tumour. C: Histopathological analysis of a tumour slice of a primary pancreatic tumour showing fluorescence, CEA expression, and microscopically localisation of tumour cells. Adapted and reprinted by permission from Springer Nature: Annals of Surgical Oncology © 201839.

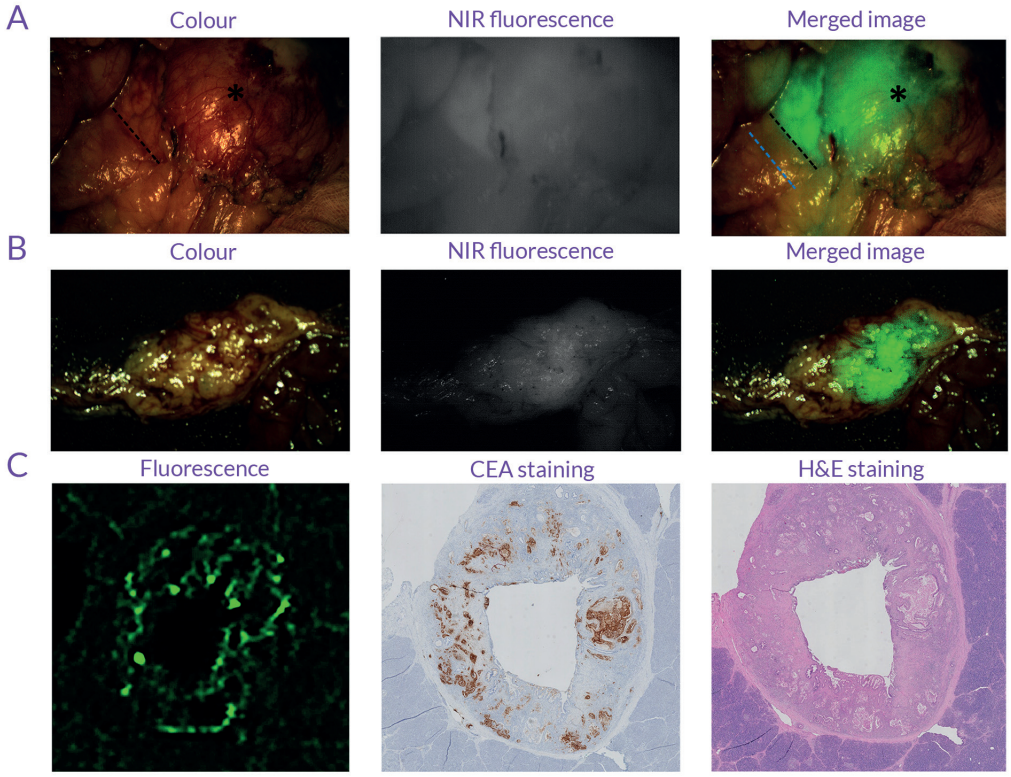

Table 2: Overview of the different (sub-) classes of targeting moieties used for the design of targeted fluorescent contrast agents and key-elements to consider towards clinical application and implementation.

	mAbs	Ab-Fragments		Protein Scaffolds	Peptides	Small Molecules
		High MW	Low MW			
Size	150 kDa	80 kDa	15 - 55 kDa	3 – 10 kDa	0.5 - 2 kDa	0.5 – 1 kDa
Delayed scanning time	Several days	One to several days	One to several hours	1 – 3 h	1 – 24 h	1 – 24 h
Tissue penetration	+/-	+	+/++	++	+++	+++
Platform technology	Yes	Yes	Yes	Yes	No	No
Generation strategy	Immunization	Immunization	Immunization	Random mutagenesis - Rational design	Rational design	Rational design
Routine production method	Fermentation	Fermentation	Fermentation	Fermentation/ Chemical Synthesis	Chemical Synthesis	Chemical Synthesis
(cGMP) Production Cost	€€€	€€€	€€€	€€€/€	€	€
Subclasses applied in fluorescence-guided surgery		Minibody	Fab, Diabody, scFv, Nanobody	Affibody, Centyrin, Knottin	Linear, Cyclic	

References

1. Tilly C, Lefevre JH, Svrcek M, et al. R1 rectal resection: look up and don't look down. Ann Surg 2014; 260(5): 794-9; discussion 9-800.
2. Wong LS, McMahon J, Devine J, et al. Influence of close resection margins on local recurrence and disease-specific survival in oral and oropharyngeal carcinoma. Br J Oral Maxillofac Surg 2012; 50(2): 102-8.
3. Esposito I, Kleeff J, Bergmann F, et al. Most pancreatic cancer resections are R1 resections. Ann Surg Oncol 2008; 15(6): 1651-60.
4. Vos EL, Gaal J, Verhoef C, Brouwer K, van Deurzen CHM, Koppert LB. Focally positive margins in breast conserving surgery: Predictors, residual disease, and local recurrence. Eur J Surg Oncol 2017; 43(10): 1846-54.
5. Stammes MA, Bugby SL, Porta T, et al. Modalities for image- and molecular-guided cancer surgery. Br J Surg 2018; 105(2): e69-e83.
6. Gioux S, Choi HS, Frangioni JV. Image-guided surgery using invisible near-infrared light: fundamentals of clinical translation. Mol Imaging 2010; 9(5): 237-55.
7. van Manen L, Handgraaf HJM, Diana M, et al. A practical guide for the use of indocyanine green and methylene blue in fluorescence-guided abdominal surgery. J Surg Oncol 2018; 118(2): 283-300.
8. Stummer W, Pichlmeier U, Meinel T, et al. Fluorescence-guided surgery with 5-aminolevulinic acid for resection of malignant glioma: a randomised controlled multicentre phase III trial. Lancet Oncol 2006; 7(5): 392-401.
9. Grossman HB, Stenzl A, Fradet Y, et al. Long-term decrease in bladder cancer recurrence with hexaminolevulinate enabled fluorescence cystoscopy. J Urol 2012; 188(1): 58-62.
10. Hadjipanayis CG, Widhalm G, Stummer W. What is the Surgical Benefit of Utilizing 5-Aminolevulinic Acid for Fluorescence-Guided Surgery of Malignant Gliomas? Neurosurgery 2015; 77(5): 663-73.
11. Vahrmeijer AL, Hutteman M, van der Vorst JR, van de Velde CJ, Frangioni JV. Image-guided cancer surgery using near-infrared fluorescence. Nat Rev Clin Oncol 2013; 10(9): 507-18.
12. van Dam GM, Themelis G, Crane LM, et al. Intraoperative tumour-specific fluorescence imaging in ovarian cancer by folate receptor-alpha targeting: first in-human results. Nat Med 2011; 17(10): 1315-9.
13. Kennedy GT, Okusanya OT, Keating JJ, et al. The Optical Biopsy: A Novel Technique for Rapid Intraoperative Diagnosis of Primary Pulmonary Adenocarcinomas. Ann Surg 2015; 262(4): 602-9.
14. Okusanya OT, DeJesus EM, Jiang JX, et al. Intraoperative molecular imaging can identify lung adenocarcinomas during pulmonary resection. J Thorac Cardiovasc Surg 2015; 150(1): 28-35 e1.
15. Tummers QR, Hoogstins CE, Gaarenstroom KN, et al. Intraoperative imaging of folate receptor alpha positive ovarian and breast cancer using the tumour specific agent EC17. Oncotarget 2016; 7(22): 32144-55.
16. Guzzo TJ, Jiang J, Keating J, et al. Intraoperative Molecular Diagnostic Imaging Can Identify Renal Cell Carcinoma. J Urol 2016; 195(3): 748-55.
17. Hoogstins CE, Tummers QR, Gaarenstroom KN, et al. A Novel Tumour-Specific Agent for Intraoperative Near-Infrared Fluorescence Imaging: A Translational Study in Healthy Volunteers and Patients with Ovarian Cancer. Clin Cancer Res 2016; 22(12): 2929-38.
18. Shum CF, Bahler CD, Low PS, et al. Novel Use of Folate-Targeted Intraoperative Fluorescence, OTL38, in Robot-Assisted Laparoscopic Partial Nephrectomy: Report of the First Three Cases. J Endourol Case Rep 2016; 2(1): 189-97.
19. Predina JD, Newton AD, Keating J, et al. Intraoperative Molecular Imaging Combined With Positron Emission Tomography Improves Surgical Management of Peripheral Malignant Pulmonary Nodules. Ann Surg 2017; 266(3): 479-88.
20. Predina JD, Newton A, Connolly C, Singhal S. Folate receptor-targeted molecular imaging improves identification of malignancy during pulmonary resection: a case report. J Cardiothorac Surg 2017; 12(1): 110.
21. Predina JD, Newton AD, Xia L, et al. An open label trial of folate receptor-targeted intraoperative molecular imaging to localize pulmonary squamous cell carcinomas. Oncotarget 2018; 9(17): 13517-29.
22. Predina JD, Newton AD, Keating J, et al. A Phase I Clinical Trial of Targeted Intraoperative Molecular Imaging for Pulmonary Adenocarcinomas. Ann Thorac Surg 2018; 105(3): 901-8.
23. Predina JD, Newton AD, Connolly C, et al. Identification of a Folate Receptor-Targeted Near-Infrared Molecular Contrast Agent to Localize Pulmonary Adenocarcinomas. Mol Ther 2018; 26(2): 390-403.
24. Predina JD, Newton A, Corbett C, et al. Localization of Pulmonary Ground-Glass Opacities with Folate Receptor-Targeted Intraoperative Molecular Imaging. J Thorac Oncol 2018; 13(7): 1028-36.
25. Pierce JT, Cho SS, Nag S, et al. Folate Receptor Overexpression in Human and Canine Meningiomas-Immunohistochemistry and Case Report of Intraoperative Molecular Imaging. Neurosurgery 2018.
26. Boogerd LSF, Hoogstins CES, Gaarenstroom KN, et al. Folate receptor-alpha targeted near-infrared fluorescence imaging in high-risk endometrial cancer patients: a tissue microarray and clinical feasibility study. Oncotarget 2018; 9(1): 791-801.
27. Harlaar NJ, Koller M, de Jongh SJ, et al. Molecular fluorescence-guided surgery of peritoneal carcinomatosis of colorectal origin: a single-centre feasibility study. The Lancet Gastroenterology & Hepatology 2016; 1(4): 283-90.
28. Lamberts LE, Koch M, de Jong JS, et al. Tumour-Specific Uptake of Fluorescent Bevacizumab-IRDye800CW Microdosing in Patients with Primary Breast Cancer: A Phase I Feasibility Study. Clin Cancer Res 2017; 23(11): 2730-41.
29. de Boer E, Warram JM, Tucker MD, et al. In Vivo Fluorescence Immunohistochemistry: Localization of Fluorescently Labeled Cetuximab in Squamous Cell Carcinomas. Sci Rep 2015; 5: 10169.
30. Rosenthal EL, Warram JM, de Boer E, et al. Safety and Tumour Specificity of Cetuximab-IRDye800 for Surgical Navigation in Head and Neck Cancer. Clin Cancer Res 2015; 21(16): 3658-66.
31. Rosenthal EL, Moore LS, Tipirneni K, et al. Sensitivity and Specificity of Cetuximab-IRDye800CW to Identify Regional Metastatic Disease in Head and Neck Cancer. Clin Cancer Res 2017; 23(16): 4744-52.
32. Gao RW, Teraphongphom N, de Boer E, et al. Safety of panitumumab-IRDye800CW and cetuximab-IRDye800CW for

fluorescence-guided surgical navigation in head and neck cancers. Theranostics 2018; 8(9): 2488-95.
33. Tummers WS, Miller SE, Teraphongphom NT, et al. Intraoperative Pancreatic Cancer Detection using Tumour-Specific Multimodality Molecular Imaging. Ann Surg Oncol 2018; 25(7): 1880-8.
34. Tummers WS, Miller SE, Teraphongphom NT, et al. Detection of visually occult metastatic lymph nodes using molecularly targeted fluorescent imaging during surgical resection of pancreatic cancer. HPB (Oxford) 2019.
35. Miller SE, Tummers WS, Teraphongphom N, et al. First-in-human intraoperative near-infrared fluorescence imaging of glioblastoma using cetuximab-IRDye800. J Neurooncol 2018; 139(1): 135-43.
36. Gao RW, Teraphongphom NT, van den Berg NS, et al. Determination of Tumour Margins with Surgical Specimen Mapping Using Near-Infrared Fluorescence. Cancer Res 2018; 78(17): 5144-54.
37. van Keulen S, van den Berg NS, Nishio N, et al. Rapid, non-invasive fluorescence margin assessment: Optical specimen mapping in oral squamous cell carcinoma. Oral Oncol 2019; 88: 58-65.
38. van Keulen S, Nishio N, Fakurnejad S, et al. The clinical application of fluorescence-guided surgery in head and neck cancer. J Nucl Med 2019; publised online Feb 7. DOI:10.2967/jnumed.118.222810.
39. Boogerd LSF, Hoogstins CES, Schaap DP, et al. Safety and effectiveness of SGM-101, a fluorescent antibody targeting carcinoembryonic antigen, for intraoperative detection of colorectal cancer: a dose-escalation pilot study. The Lancet Gastroenterology & Hepatology 2018; 3(3): 181-91.
40. Hoogstins CES, Boogerd LSF, Sibinga Mulder BG, et al. Image-Guided Surgery in Patients with Pancreatic Cancer: First Results of a Clinical Trial Using SGM-101, a Novel Carcinoembryonic Antigen-Targeting, Near-Infrared Fluorescent Agent. Ann Surg Oncol 2018; 25(11): 3350-7.
41. Hekman MC, Rijpkema M, Muselaers CH, et al. Tumour-targeted Dual-modality Imaging to Improve Intraoperative Visualization of Clear Cell Renal Cell Carcinoma: A First in Man Study. Theranostics 2018; 8(8): 2161-70.
42. Li D, Zhang J, Chi C, et al. First-in-human study of PET and optical dual-modality image-guided surgery in glioblastoma using (68)Ga-IRDye800CW-BBN. Theranostics 2018; 8(9): 2508-20.
43. Dintzis SM, Hansen S, Harrington KM, et al. Real-time Visualization of Breast Carcinoma in Pathology Specimens From Patients Receiving Fluorescent Tumour-Marking Agent Tozuleristide. Arch Pathol Lab Med 2018.
44. Whitley MJ, Cardona DM, Lazarides AL, et al. A mouse-human phase 1 co-clinical trial of a protease-activated fluorescent probe for imaging cancer. Sci Transl Med 2016; 8(320): 320ra4.
45. Smith BL, Gadd MA, Lanahan CR, et al. Real-time, intraoperative detection of residual breast cancer in lumpectomy cavity walls using a novel cathepsin-activated fluorescent imaging system. Breast Cancer Res Treat 2018; 171(2): 413-20.
46. Unkart JT, Chen SL, Wapnir IL, Gonzalez JE, Harootunian A, Wallace AM. Intraoperative Tumour Detection Using a Ratiometric Activatable Fluorescent Peptide: A First-in-Human Phase 1 Study. Ann Surg Oncol 2017; 24(11): 3167-73.
47. van Leeuwen FW, Valdés-Olmos R, Buckle T, Vidal-Sicart S. Hybrid surgical guidance based on the integration of radionuclear and optical technologies. Br J Radiol 2016; 89: 20150797
48. Brouwer OR, Buckle T, Vermeeren L, et al. Comparing the hybrid fluorescent-radioactive tracer indocyanine green-99mTc-nanocolloid with 99mTc-nanocolloid for sentinel node identification: a validation study using lymphoscintigraphy and SPECT/CT. J Nucl Med 2012; 53(7): 1034-40.
49. KleinJan GH, van Werkhoven E, van den Berg NS, et al. The best of both worlds: a hybrid approach for optimal pre- and intraoperative identification of sentinel lymph nodes. Eur J Nucl Med Mol Imaging 2018; 45(11): 1915-25.
50. Schottelius M, Wurzer A, Wissmiller K, et al. Synthesis and Preclinical Characterization of the PSMA-Targeted Hybrid Tracer PSMA-I&F for Nuclear and Fluorescence Imaging of Prostate Cancer. J Nucl Med 2019; 60(1): 71-8.
51. Odenthal J, Rijpkema M, Bos D, et al. Targeting CD44v6 for fluorescence-guided surgery in head and neck squamous cell carcinoma. Sci Rep 2018; 8(1): 10467.
52. Boonstra MC, Van Driel PB, Keereweer S, et al. Preclinical uPAR-targeted multimodal imaging of locoregional oral cancer. Oral Oncol 2017; 66: 1-8.
53. Lwin TM, Miyake K, Murakami T, et al. Fluorescent humanized anti-CEA antibody specifically labels metastatic pancreatic cancer in a patient-derived orthotopic xenograft (PDOX) mouse model. Oncotarget 2018; 9(99): 37333-42.
54. van Driel PB, Boonstra MC, Prevoo HA, et al. EpCAM as multi-tumour target for near-infrared fluorescence guided surgery. BMC Cancer 2016; 16(1): 884.
55. Warram JM, de Boer E, Moore LS, et al. A ratiometric threshold for determining presence of cancer during fluorescence-guided surgery. J Surg Oncol 2015; 112(1): 2-8.
56. Xenataki KT, Oliveira S, van Bergen en Henegouwen PM. Antibody or Antibody Fragments- Implications for Molecular Imaging and Targeted Therapy of Solid Tumours. Frontiers in Immunology 2017; doi: 10.3389/ mmu.2017.01287.
57. Sonn GA, Behesnilian AS, Jiang ZK, et al. Fluorescent Image-Guided Surgery with an Anti-Prostate Stem Cell Antigen (PSCA) Diabody Enables Targeted Resection of Mouse Prostate Cancer Xenografts in Real Time. Clin Cancer Res 2016; 22(6): 1403-12.
58. Zhang M, Kobayashi N, Zettlitz KA, et al. Near-Infrared Dye-Labeled Anti-Prostate Stem Cell Antigen Minibody Enables Real-Time Fluorescence Imaging and Targeted Surgery in Translational Mouse Models. Clinical Cancer Research 2019; 25(1): 188-200.
59. Krasniqi A, D'Huyvetter M, Devoogdt N, et al. Same-Day Imaging Using Small Proteins: Clinical Experience and Translational Prospects in Oncology. J Nucl Med 2018; 59(6): 885-91.
60. Debie P, Van Quathem J, Hansen I, et al. Effect of Dye and Conjugation Chemistry on the Biodistribution Profile of Near-Infrared-Labeled Nanobodies as Tracers for Image-Guided Surgery. Mol Pharm 2017; 14(4): 1145-53.
61. Boogerd LSF, Boonstra MC, Prevoo HAJM, et al. Fluorescence-guided tumour detection with a novel anti-EpCAM targeted antibody fragment: Preclinical validation. Surgical Oncology 2019; 28: 1-8.
62. Debie P, Vanhoeij M, Poortmans N, et al. Improved Debulking of Peritoneal Tumour Implants by Near-Infrared Fluorescent Nanobody Image Guidance in an Experimental Mouse Model. Mol Imaging Biol 2018; 20(3): 361-7.

63. van Brussel AS, Adams A, Oliveira S, et al. Hypoxia-Targeting Fluorescent Nanobodies for Optical Molecular Imaging of Pre-Invasive Breast Cancer. Mol Imaging Biol 2016; 18(4): 535-44.
64. Mahalingam SM, Dudkin VY, Goldberg S, et al. Evaluation of a Centyrin-Based Near-Infrared Probe for Fluorescence-Guided Surgery of Epidermal Growth Factor Receptor Positive Tumours. Bioconjug Chem 2017; 28(11): 2865-73.
65. Tummers WS, Kimura RH, Abou-Elkacem L, et al. Development and Preclinical Validation of a Cysteine Knottin Peptide Targeting Integrin alphavbeta6 for Near-infrared Fluorescent-guided Surgery in Pancreatic Cancer. Clin Cancer Res 2018; 24(7): 1667-76.
66. Samkoe KS, Gunn JR, Marra K, et al. Toxicity and Pharmacokinetic Profile for Single-Dose Injection of ABY-029: a Fluorescent Anti-EGFR Synthetic Affibody Molecule for Human Use. Mol Imaging Biol 2017; 19(4): 512-21.
67. de Souza AL, Marra K, Gunn J, et al. Fluorescent Affibody Molecule Administered In Vivo at a Microdose Level Labels EGFR Expressing Glioma Tumour Regions. Mol Imaging Biol 2017; 19(1): 41-8.
68. Xu H, Bandari RP, Lee L, et al. Design, Synthesis, and in Vitro and in Vivo Evaluation of High Affinity and Specificity Near-Infrared Fluorescent Bombesin Antagonists for Tumour Imaging. J Med Chem 2018; 61(17): 7657-70.
69. Handgraaf HJM, Boonstra MC, Prevoo H, et al. Real-time near-infrared fluorescence imaging using cRGD-ZW800-1 for intraoperative visualization of multiple cancer types. Oncotarget 2017; 8(13): 21054-66.
70. Choi HS, Gibbs SL, Lee JH, et al. Targeted zwitterionic near-infrared fluorophores for improved optical imaging. Nat Biotechnol 2013; 31(2): 148-53.
71. Hyun H, Owens EA, Narayana L, et al. Central C-C Bonding Increases Optical and Chemical Stability of NIR Fluorophores. RSC Adv 2014; 4(102): 58762-8.
72. Koch M, Symvoulidis P, Ntziachristos V. Tackling standardization in fluorescence molecular imaging. Nature Photonics 2018; 12(9): 505-15.
73. Valdes PA, Angelo JP, Choi HS, Gioux S. qF-SSOP: real-time optical property corrected fluorescence imaging. Biomed Opt Express 2017; 8(8): 3597-605.
74. Koller M, Qiu SQ, Linssen MD, et al. Implementation and benchmarking of a novel analytical framework to clinically evaluate tumour-specific fluorescent tracers. Nat Commun 2018; 9(1): 3739.
75. Tummers WS, Warram JM, van den Berg NS, et al. Recommendations for reporting on emerging optical imaging agents to promote clinical approval. Theranostics 2018; 8(19): 5336-47.
76. Pogue BW, Zhu TC, Ntziachristos V, et al. Fluorescence-guided surgery and intervention - An AAPM emerging technology blue paper. Med Phys 2018; 45(6): 2681-8.
77. Braga M, Vignali A, Zuliani W, Frasson M, Di Serio C, Di Carlo V. Laparoscopic versus open colorectal surgery: cost-benefit analysis in a single-center randomized trial. Ann Surg 2005; 242(6): 890-5, discussion 5-6.